Wallace, L.M., Saffer, D.M., Barnes, P.M., Pecher, I.A., Petronotis, K.E., LeVay, L.J., and the Expedition 372/375 Scientists
Proceedings of the International Ocean Discovery Program Volume 372B/375
publications.iodp.org

Data report: marine tephra compositions in proximal and distal drill cores, IODP Expeditions 375, 372, and 329, ODP Leg 181, and DSDP Leg 90, offshore New Zealand, Southwest Pacific[1]

Katharina Pank,[2] Steffen Kutterolf,[2] Jenni L. Hopkins,[3] Kuo-Lung Wang,[4,5] Hao-Yang Lee[5]

[1] Pank, K., Kutterolf, S., Hopkins, J.L., Wang, K.-L., and Lee, H.-Y., 2023. Data report: marine tephra compositions in proximal and distal drill cores, IODP Expeditions 375, 372, and 329, ODP Leg 181, and DSDP Leg 90, offshore New Zealand, Southwest Pacific. In Wallace, L.M., Saffer, D.M., Barnes, P.M., Pecher, I.A., Petronotis, K.E., LeVay, L.J., and the Expedition 372/375 Scientists, Hikurangi Subduction Margin Coring, Logging, and Observatories. Proceedings of the International Ocean Discovery Program, 372B/375: College Station, TX (International Ocean Discovery Program). https://doi.org/10.14379/iodp.proc.372B375.210.2023
[2] GEOMAR Helmholtz Centre for Ocean Research Kiel, Germany. Correspondence author: **kpank@geomar.de**
[3] School of Geography Environment and Earth Science, Victoria University of Wellington, New Zealand.
[4] Institute of Earth Sciences, Academia Sinica, Taiwan.
[5] Department of Geosciences, National Taiwan University, Taiwan.

Contents

Keywords
International Ocean Discovery Program, IODP, *JOIDES Resolution*, Expedition 375, Hikurangi Subduction Margin Coring, Logging, and Observatories, Expedition 372, Expedition 329, Leg 181, Leg 90

Supplementary material

References (RIS)

MS 372B375-210
Received 8 December 2022
Accepted 1 February 2023
Published 21 April 2023

Abstract

We report on a total of 1005 samples analyzed for major and trace element compositions from marine sediments drilled along the Hikurangi subduction zone and within the incoming Pacific plate. The samples are from International Ocean Discovery Program Expeditions 375 and 372; Integrated Ocean Drilling Program Expedition 329; Ocean Drilling Program Leg 181; and Deep Sea Drilling Project Leg 90.

All 1005 samples, resulting in a total number of ~20,200 individual measurements, were analyzed for major element compositions with the electron microprobe. A subset of 419 samples, resulting in a total number of ~1820 individual glass shard analyses, were analyzed for trace element compositions using the laser ablation-inductively coupled plasma-mass spectrometer. In total, ~640 samples were identified as primary ash layers based on their homogeneous geochemistry, visual appearance in the core pictures, and high amount of volcanic glass. Based on the biostratigraphy presented in the cruise reports and subsequent work, we can distinguish between Quaternary- and Neogene-derived tephras. The tephra layers of Quaternary age are mostly of rhyolitic composition with occasional andesitic, dacitic, and trachytic glass shards. The Neogene tephras are mostly of basaltic andesite, andesitic, and rhyolitic composition, with a few basaltic and trachytic tephras. Tephras of both age groups follow the calc-alkaline series trend with a tendency to shift into the high-K calc-alkaline series for tephras with >70 wt% SiO_2.

1. Introduction

International Ocean Discovery Program (IODP) Expedition 375, together with Expedition 372, was initiated to investigate regularly recurring slow slip events (SSEs) along the northern Hikurangi subduction margin. These SSEs recur every 1–2 y over a period of 2–3 weeks at <2–15 km below the seafloor (see **Saffer et al.**, 2019, and references therein) and are linked to several factors that were investigated during Expeditions 375 and 372. The main objectives of Expedition 375 were the deformation rate and associated chemical and physical properties throughout entire slow slip cycles, the lithologic and structural character of active faults, and the material that is transported to the SSE source region. Expedition 372 also focused on landslides potentially involving gas hydrates along the Hikurangi margin. Together, both expeditions aimed to investigate the

character and properties of SSEs and their relationship with earthquakes along the subduction interface. Pecher et al. (2018) found that earthquakes along the Hikurangi margin influence sedimentation on both the slope and the incoming plate either by remobilizing large stratigraphically intact blocks of sediments or frequent triggering of turbidity currents. Here, the amount and character of the sediments involved play a fundamental role. In the case of New Zealand, the sediments are strongly influenced by the high volcanological input from the Taupõ Volcanic Zone (Quaternary) and Coromandel Volcanic Zone (Neogene) in the form of discrete tephra layers or dispersed ash. These tephra layers may be used to help characterize the timing and distribution of submarine slides along the Hikurangi margin. For this, a tephrochronostratigraphic framework based on correlations to well-dated onshore deposits (e.g., through geochemical fingerprinting) or direct age dating (e.g., radiometric techniques) is required and will help to date sediment sequences and potential submarine slides. The investigation and understanding of earthquakes, submarine slides, and volcanism and their potential links is crucial not only to New Zealand but globally.

We here present individual glass shard analyses of major and trace elements of (discrete) tephra layers building the foundation of the tephrostratigraphic framework back to the Miocene. The major and trace element compositions of tephras generally provide information about the depositional character (e.g., primary versus reworked origin) of the layers (e.g., Freundt et al., 2022) and allow for correlation between sites and onshore reference data. The compositional data provided in this report will be the foundation for upcoming publications focusing on the compositional and temporal tephrostratigraphic framework during the Quaternary and Neogene. Upcoming publications will also include correlations between individual holes, sites, and terrestrial reference deposits and new age models based on sedimentation rates verified by prominent marker horizons, finally contributing to a tephrochronostratigraphic framework for New Zealand.

1.1. Expedition 372/375 sites

The majority of investigated tephras were retrieved from four Expedition 375 sites (U1518–U1520 and U1526) and one Expedition 372 site (U1517). Tephras from Holes U1519C–U1519E were recovered during Expedition 375, but the site was initiated with logging while drilling operations during Expedition 372. Expedition 375 sites are aligned on a northwest–southeast transect offshore of Gisborne, New Zealand, covering distinct areas of the subduction margin (Figure **F1**).

1.1.1. Site U1519

Site U1519 (Figure **F1A**) is the northernmost drill site and is located on the shelf in the Tuaheni Basin (Figure **F1B**) about 38 km from shore at a water depth of ~1000 m (**Saffer et al.**, 2019). Calcareous nannofossils and planktonic foraminifer species indicate an age between the Holocene (base at 4.4–14.0 meters below seafloor [mbsf]) and Pleistocene (~635 mbsf) (Crundwell and Woodhouse, 2022b). Two lithostratigraphic units were identified at Site U1519 (**Barnes et al.**, 2019b). Unit I (shallower than 282.66 mbsf) consists of mud, mudstone, minor silt, and volcanic ash in a hemipelagic setting with rare dilute turbidity currents. Unit II consists of (silty) mudstone, fine to coarse sand, rare volcanic ash, and mass transport deposits in a hemipelagic setting with turbidity currents and debris flows.

1.1.2. Site U1518

Site U1518 (Figure **F1**) is located in the frontal accretionary wedge about 73 km from shore at a water depth of ~2630 m. Planktonic foraminifers and calcareous nannofossils indicate an age of Holocene–Pleistocene (Crundwell and Woodhouse, 2022b). Three lithostratigraphic units were identified (**Saffer et al.**, 2019). Unit I (divided into Subunits IA and IB) consists of silty clay/sand and sandy silt interbedded with volcanic ash in the upper 40 m and fine-grained turbidites and hemipelagic sediments deposited in a trench-floor environment (Subunit IA, lower part). Subunit IB (197.7–304.5 mbsf) consists of mudstone with siltstone, hemipelagic sediments, and fine-grained turbidites deposited in a trench-floor environment. Unit II (304.5–370.4 mbsf) consists of alternating layers of silty mudstone and sparse siltstone, with hemipelagic sediments in the lower parts. Unit III is also divided into two parts (Subunits IIIA and IIIB). The upper part of Subunit IIIA (370.4–475.7 mbsf) contains bioturbated mudstone interbedded with thin layers of (sandy)

siltstone, and the lower part contains turbidites and soft-sediment deformation (mass transport deposits). Subunit IIIB (deeper than 475.7 mbsf) consists of mudstone/siltstone interbeds.

1.1.3. Site U1520

Site U1520 (Figure **F1A**) is located on the incoming subducting Pacific plate in the Hikurangi Trough (Figure **F1B**), about 16 km east of the deformation front and ~95 km from shore at a water depth of ~3520 m. The biostratigraphy indicates a discontinuous recovery of Holocene to Late Cretaceous successions comprising several hiatus-bounded packages. Six lithostratigraphic units were identified (**Barnes et al.**, 2019c). Unit I (shallower than 110.5 mbsf) consists of hemipelagic trench-wedge facies with sand, silt, and silty sand(stones). Unit II (110.5–222.0 mbsf) is characterized as the Ruatoria slide, hemipelagic mud(stone) with silt. Unit III (222.0–509.82 mbsf) consists of hemipelagic trench-wedge facies with volcanic ash/tuff, silty sand(stone), debris flow deposits, and black mudstones. Unit IV (509.82–848.54 mbsf) consists of pelagic facies (predominantly marl), debris flow deposits, volcanic ash/tuff, and (muddy) chalk at the base. Unit V (848.45–1016.26 mbsf) is a volcaniclastic facies, and Unit VI (deeper than 1016.24 mbsf) consists of mixed lithologies such as volcaniclastic conglomerates, black mudstone, and basalts.

1.1.4. Site U1526

Site U1526, the southeasternmost drill site (Figure **F1A**), is located on the Tūranganui Knoll at a water depth of 2908 m (Figure **F1B**). The biostratigraphy indicates a varying age of the sedimentary succession from the Holocene to Late Cretaceous (Crundwell and Woodhouse, 2022b). Two lithostratigraphic units were identified (**Wallace et al.**, 2019). Unit I (shallower than 30.23 mbsf) consists of hemipelagic to biocalcareous facies of (calcareous) mud and nannofossil ooze. Unit II (deeper than 30.23 mbsf) is a volcaniclastic facies with coarse volcaniclastic sandstone, including shell hash, volcaniclastic conglomerate/breccia, and vesicular basalt, probably deposited in a shallow marine environment.

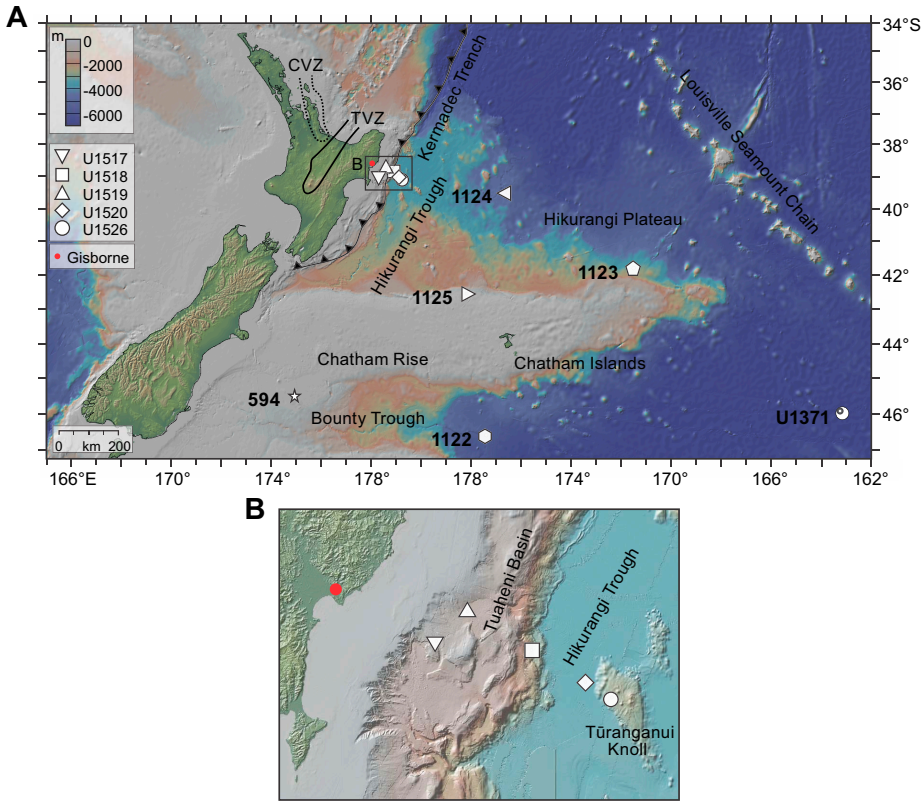

Figure F1. A. IODP, ODP, and DSDP sites and larger scale tectonic features east of New Zealand. TVZ = Taupō Volcanic Zone (solid line), CVZ = Coromandel Volcanic Zone (dotted line). B. Expedition 372 and 375 sites across the Hikurangi subduction margin with smaller scale tectonic features. Maps created with GeoMapApp, Global Multiresolution Topography Data Synthesis (GMRT) after Ryan et al. (2009).

1.1.5. Site U1517

Site U1517 (Figure **F1**) is located southwest of Site U1519 in the extensional, creeping part of the Tuaheni Landslide Complex at a water depth of about 720 m. Calcareous nannofossils and planktonic foraminifers indicate that the sedimentary sequence is of Holocene to Middle Pleistocene age (Crundwell and Woodhouse, 2022b). Five lithostratigraphic units were described (Barnes et al., 2019a). Unit I (shallower than 3 mbsf) consists of silty clay, volcaniclastic fine sand, and a sandy base. Unit II (3.0–40.74 mbsf; alternating mud and sand) and Unit III (40.74–66.38 mbsf; massive clayey silt to silty clay with alternating silt and clay, including blebs of sand and ash) comprise the Tuaheni slide mass, apparently an intact block that was mobilized from the upper slope sedimentary sequences. Unit IV (66.38–103.16 mbsf) is characterized as massive clayey silt with variable amounts of clay and volcaniclastic material with a sand bed at the base. Unit V (103.16–187.53 mbsf) is composed of alternating sand and mud intervals of massive clayey silt or silty clay, very fine grained silt, and volcaniclastic material in the form of ash/tuff layers.

1.2. Leg 181 sites

The drill sites of Expeditions 375 and 372 cover the proximal submarine area of the Hikurangi margin and trough and may contain volcaniclastic material from relatively minor eruptions with a potentially smaller geographic distribution as well as material from large eruptions with a potentially wide geographic distribution. The volcanological record in these cores, however, might be incomplete because of erosive processes and submarine slides along the shelf and margin. Additionally, it is difficult to estimate eruption sizes based on tephra layers in proximal cores only, and especially eruptions of unknown origin, which cannot be correlated to a specific source. To address these issues in future studies, we revisited distal cores from previous expeditions: Ocean Drilling Program (ODP) Leg 181 (Carter et al., 1999), Deep Sea Drilling Program (DSDP) Leg 90 (Kennett, von der Borch, et al., 1986), and Integrated Ocean Drilling Program Expedition 329 (Expedition 329 Scientists, 2011), enlarging our study area offshore of New Zealand (Figure **F1**).

Leg 181 Sites 1122–1125 are situated on the Pacific plate between ~480 and ~960 km east and southeast of Gisborne (Figure **F1**). The information given below is referenced in the Volume 181 Initial Report (Carter et al., 1999).

Sites 1123 and 1124 were previously the focus of marine tephra inventory studies (e.g., Alloway et al., 2005; Allan et al., 2008; Stevens, 2010). However, for better compatibility and to allow trace element measurements to be made accurately, we decided to resample the cores and analyze the tephra layers. This process also gives a good control on variabilities in the data sets based on different measuring protocols, allowing the data to be directly compared.

1.2.1. Site 1122

Site 1122 is located ~950 km south-southeast of Gisborne at a water depth of 4432 m on the northern bank levee of the abyssal Bounty Fan (Figure **F1**). The recovered stratigraphic sequence is mostly of Miocene to Pleistocene age, including a few meters of Holocene. Three lithostratigraphic units were identified. Unit I consists of a thick sequence of turbidites and is divided into four subunits. Unit II (386.9–550.4 mbsf) consists of bioturbated pelagic/hemipelagic sediments interspersed with current-laminated deposits, and Unit III (550.4–617.85 mbsf) contains bioturbated pelagic/hemipelagic sediments interspersed with laminated current deposits common to drift deposits.

1.2.2. Site 1123

Site 1123 (Figure **F1**) is located on the northeastern slopes of Chatham Rise about 960 km southeast of Gisborne at a water depth of 3290 m. Recovered cores range from Pleistocene to Miocene age and contain successions of clay-rich nannofossil ooze, chalk, and limestone. Four lithostratigraphic units were identified. Unit I (0–256.59 mbsf) is characterized by an interglacial–glacial cyclic sedimentation pattern of clayey nannofossil ooze and abundant to occasional tephra intercalations. Unit II (256.59–450.8 mbsf) consists of a fairly uniform lithology of chalk with tephra beds. Unit III (450.8–489 and 484–542.9 mbsf) is again characterized by an interglacial–glacial cyclic sedimentation pattern of mudstone and chalk and contains a ~7 m thick debris flow. Unit IV

(587.2–632.8 mbsf) is of Eocene/Oligocene age and consists of micritic limestone with bioturbation.

1.2.3. Site 1124

Site 1124 is located about 480 km east-southeast from Gisborne (Figure **F1**) at a water depth of 3978 m. The biostratigraphy indicates an age of Late Cretaceous to Pleistocene. Six lithostratigraphic units were described. Unit I (shallower than 300 mbsf) is divided into three subunits and consists of a succession of interbedded ooze, chalk, and silty clay with frequent tephra layers of varying thickness. Unit II (~302–411 mbsf) consists of nannofossil chalk with interbeds of clay-bearing nannofossil chalk containing a biosiliceous component. Unit III (~411–419 mbsf) is composed of a uniform clayey nannofossil chalk. Unit IV (~419–429 mbsf) marks an abrupt change to mudstones. Unit V (~429–467 mbsf) consists of nannofossil-bearing mudstone and isolated beds of nannofossil chalk. Unit VI (~467–473 mbsf) consists of nannofossil-bearing mudstones with chert lenses.

1.2.4. Site 1125

Site 1125 is located about 550 km southeast of Gisborne (Figure **F1**) on the north slope of Chatham Rise at a water depth of 1360 m. Two lithostratigraphic units of Miocene to Pleistocene age were recovered. Unit I (shallower than 245.2 mbsf) represents an interglacial–glacial cyclic sedimentation pattern of alternating nannofossil ooze and silty clay and is divided into two subunits. Unit II (245.2–331.5 mbsf) consists of mainly clayey nannofossil chalk.

1.3. Leg 90 site

1.3.1. Site 594

Leg 90 Site 594 is located 790 km south of Gisborne at the southern margin of the Chatham Rise, east of South Island, New Zealand (Figure **F1**). Two lithostratigraphic units were recognized. Unit I consists of alternating pelagic and hemipelagic lithofacies with nannofossil ooze. Unit II consists of pelagic facies with nannofossil ooze and nannofossil chalk (Kennett, von der Borch, et al., 1986).

1.4. Expedition 329 site

1.4.1. Site U1371

Expedition 329 Site U1371 is the southeasternmost drill site and is located about ~1750 km southeast of Gisborne and about 840 km southeast of Site 1123 (Figure **F1**) at a water depth of about 5301 m. The recovered sediments consist of diatom ooze and pelagic clay and are divided into two units. Unit I consists of ooze with varying diatom and clay content and numerous ash layers. Unit II consists of clay and zeolite (Expedition 329 Scientists, 2011).

By combining the selected drill sites, including both the proximal subduction margin and distal Pacific plate, our research and especially the data report presented here offer a unique opportunity to investigate an unprecedented and holistic view of the volcanic activity of New Zealand and the surrounding volcanic areas (e.g., the Kermadec arc) since the Miocene.

Additionally, the elaboration and interpretation of the data will allow us to fill or verify gaps in the well-constrained Quaternary Taupõ Volcanic Zone volcanic activity by including tephras of smaller eruptions, which are more likely to be eroded or obscured in the geologic record on land, and thus not described so far.

2. Methods

2.1. Sampling

The cores retrieved during Expeditions 375 and 372 were sampled for visible tephra deposits during the expedition. Visual core descriptions, including lithologic and sedimentary features, and smear slide analyses were used to identify intervals of interest indicating (primary) tephra layers. The visual description of the cores was done on archive-half sections, whereas samples were taken

from the working-half sections. The cores from Leg 181, Expedition 329, and Leg 90 were resampled at the IODP Gulf Coast Repository (USA).

2.2. Laboratory preparation

The marine ash samples were wet-sieved into different grain size fractions (63–125, 125–250, >250, and if necessary, 32–63 µm). Lithified samples from deeper sections of Site U1520 were disaggregated in an ultrasonic bath prior to sieving. The fraction 63–125 µm was further used for compositional analysis of glass shards with the electron microprobe (EMP) by embedding twelve samples with the two-component epoxy resin, Araldite, into one 1 inch predrilled acrylic mount that has twelve 2 mm-ø holes. After approximately 48 h at about 50°C in the drying cabinet, the sample surfaces were polished with polishing paste of 9, 3, and 1 µm grain size and then carbon-coated to provide discharge of the electrons during EMP analysis. For laser ablation-inductively coupled plasma-mass spectrometry (LA-ICP-MS) analyses, both fractions 63–125 and 125–250 µm were embedded and further processed as described above.

2.3. Electron microprobe analyses

A total of 1005 samples, resulting in ~20,200 individual measurements (15–20 glass shards per sample), were analyzed for major and minor elements (Na_2O, K_2O, FeO, SiO_2, TiO_2, MgO, MnO, Al_2O_3, and P_2O_5) using a JEOL JXA 8200 wavelength dispersive EMP at GEOMAR Helmholtz Centre for Ocean Research Kiel utilizing the methods of Kutterolf et al. (2011). An internal, calibrated measuring program was used based on international standard material and a 6 nA strong and 10 µm wide electron minimized sodium loss. Oxide concentrations were determined using the ZAF correction method. The accuracy was monitored with repeated measurements every 80 individual glass shard measurements using the standards Lipari (Obsidian rhyolite; Hunt and Hill, 2001) and VGA99 (basalt from Makaopuhi Lava Lake; Jarosewich et al., 1980). The resulting standard deviations are generally better than 0.5% for major elements and <0.3% for minor elements. Analyses with <90 wt% total oxides were excluded from the data set to avoid possible alteration effects on the results. However, exceptions were made for analyses of the presumably oldest samples (e.g., Site U1520), where data acquisition was difficult, most likely because of advanced dehydration related to the older age. Accidentally measured microcrystals (e.g., highly increased Al_2O_3 content) were excluded from the data set as well. The data was normalized to 100% to eliminate possible effects of minor postdepositional hydration and/or deviations of the electron beam (e.g., defocused beam). All resulting major and minor element data are listed in ELEMENT in **Supplementary material**.

2.4. Laser ablation-inductively coupled plasma-mass spectrometry

A total of 419 tephra layers, selected (1) for the presumably major eruptive events (e.g., largest thicknesses), (2) equally throughout the stratigraphies to cover compositional changes with time, and (3) where correlation attempts will need clarification or proof using trace elements, were analyzed for trace element concentrations, resulting in a total number of ~1820 glass shard measurements (3–6 glass shards per sample). The samples were analyzed at the Institute of Earth Sciences (Taiwan) following the methods described in Kutterolf et al. (2021) using a Photon Machines Analyte G2 (193 nm) excimer laser ablation system linked to a high-resolution inductively coupled plasma–mass spectrometer (ICP-MS) (Agilent 7900). The spot size was set to 24–30 µm using 5–10 J/cm^2 energy density at 4–10 Hz repetition rate. Blank acquisition was 45 s, followed by typical ablation times of ~75 s. Data reduction was performed using GLITTER software (version 4.0) (van Achterberg et al., 2001) immediately following each ablation analysis. Individual calcium and silica concentrations for each analyzed glass shard of the samples, previously measured with EMP, were used as internal standard to calibrate the trace element analyses. Accuracy was monitored with repeated measurements of the international glass standard BCR-2G after every tenth sample measurement. The repeated measurement of the standard material assured the correction of matrix effects and signal drift of the LA-ICP-MS just as it monitors the differences in the ablation efficiency between sample and reference material (Günther et al., 1999). The reference material NIST SRM612 was needed for external calibration (Norman et al., 1996; Jochum et al., 2011). The detection limit is <100 ppb for most trace elements and around 10 ppb for rare earth elements. The

analytical precision compared to the international glass standard BCR-2G is generally better than 10% for most trace elements (see all resulting trace element data in **Supplementary material**).

3. Results

Of 1005 investigated ash-bearing samples, ~640 samples are characterized as primary ash layers because of (1) their characteristic and usually homogeneous composition in major and trace elements, (2) their visual appearance in the core pictures, and (3) volcanic glass being the dominant component. Because of the large number of investigated samples, we distinguish between tephras of the Quaternary and tephras of the Neogene. We refer to the individual cruise reports and therein included biostratigraphy with resulting age models for basic details and to more recent studies (e.g., Carter et al., 2004; Alloway et al., 2005; Crundwell and Woodhouse, 2022b, 2022a) for revised age models of Expedition 372/375 and Leg 181. Based on the established and partly revised age models for the marine sediments, we identified ~330 primary tephra layers of Quaternary age and ~310 of Neogene age (Figures **F2**, **F3**). The most continuous tephra records, covering the entire age range from recent to Neogene, were recovered from Sites U1520 and 1124 (Figure **F1**).

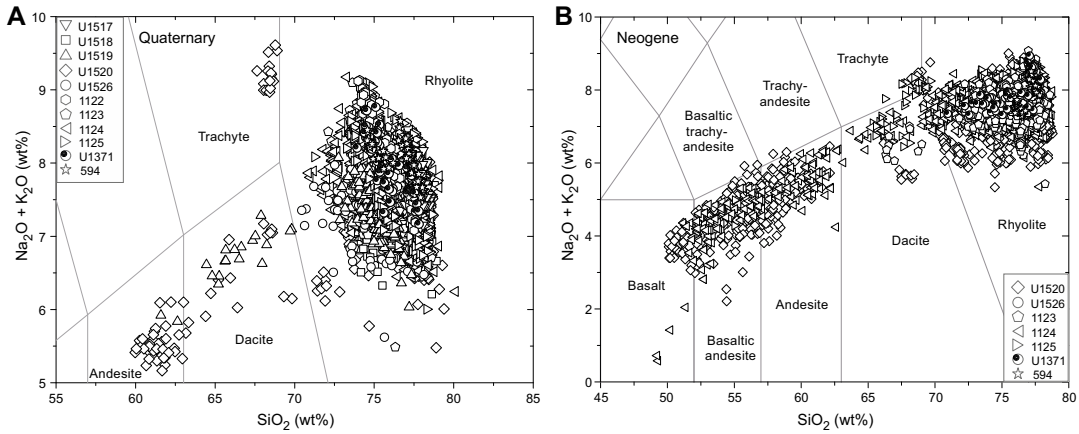

Figure F2. Total alkali vs. silica diagrams after Le Maitre et al. (2002) for the (A) Quaternary and (B) Neogene. The majority of tephras, independent of their age, are rhyolitic. Basaltic, dacitic, and trachytic glass shards are rare in the Quaternary but common in the Neogene (especially present in Sites U1520, 1123, and 1124). Shown are individual measurements of glass shards.

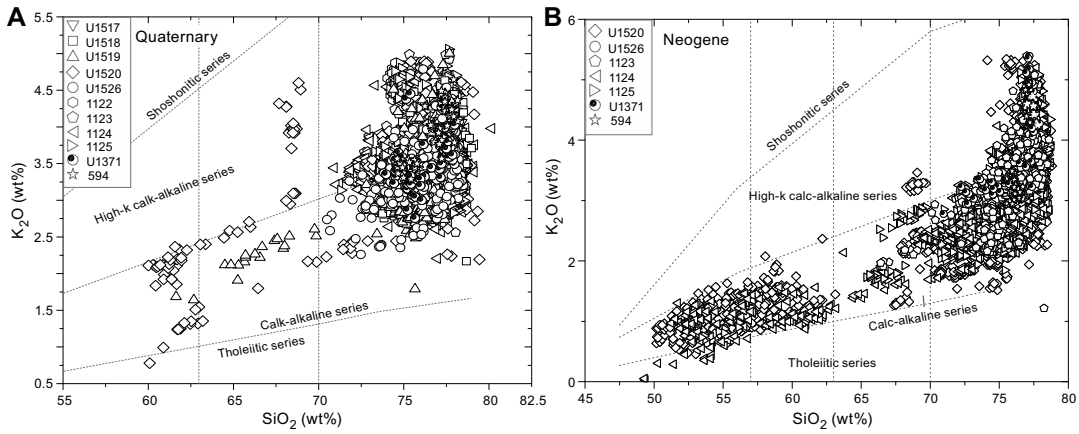

Figure F3. K_2O vs. SiO_2 classification diagram after Peccerillo and Taylor (1976) for the (A) Quaternary and (B) Neogene. Quaternary glass shards follow the calc-alkaline and high-K calc-alkaline series, with one glass shard of tholeiitic character. Neogene glass shards mostly follow the calc-alkaline series, a few glass shards straddle along the boundary between tholeiitic series and calc-alkaline series and silica-rich glass shards (>75 wt%) tend toward and plot within the high-K calc-alkaline series.

Following the total alkali versus silica diagram after Le Maitre et al. (2002), New Zealand's volcanism produced basaltic to trachytic and rhyolitic compositions (Figure **F2**) since the Neogene. The tephra layers corresponding to Quaternary age (Figure **F2A**) are predominantly rhyolitic, and the majority show SiO_2 between ~72.5 and 78 wt% and $Na_2O + K_2O$ of ~6.5–9 wt%. Dacitic and andesitic glass shards ranging ~60–63 wt% SiO_2 and 5–6 wt% $Na_2O + K_2O$ and trachytic glass shards with high alkali concentrations (≥8.8 wt%) occur rarely (Figure **F2A**). Neogene glass shards have a broader compositional range from basaltic to rhyolitic (Figure **F2B**), and the majority of tephras are basaltic andesites to andesites and rhyolites with rare low alkali (~8 wt%) trachytic glass shards. The Neogene rhyolitic compositional field is slightly broader than shown by Quaternary-derived tephras, with ~70–78 wt% SiO_2 and 6–9 wt% $Na_2O + K_2O$.

The K_2O classification diagram after Peccerillo and Taylor (1976) shows that the majority of investigated glass shards follow the calc-alkaline series, with an increase in K_2O for glass shards >70 wt% SiO_2 and minor trachytic glass shards (Figure **F3**) corresponding to the high-K calc-alkaline series. Few glass shards with <0.5 wt% K_2O and <62.5 wt% SiO_2 fall within the tholeiitic series (Figure **F3**). Although Quaternary and Neogene tephras show a similar composition, the majority of Neogene-derived glass shards fall into the calc-alkaline series, with a tail-like trend into the high-K calc-alkaline field for glass shards with >75 wt% SiO_2 (Figure **F3B**). Quaternary-derived high-SiO_2 glass shards are roughly equally distributed between the calc-alkaline and high-K calc-alkaline field (Figure **F3A**). Glass shards with 60–70 wt% SiO_2 follow the calc-alkaline series, straddle around the division line to the high-K calc-alkaline field or plot within the latter. Two individual glass shards tend toward or plot within the tholeiitic series (Figure **F3A**) and are the result of a slightly geochemically zoned, silica-poor tephra layer.

4. Acknowledgments

This study focuses on samples and data provided by IODP, as well as the Integrated Ocean Drilling Program, ODP, and DSDP. The excellent efforts of all participating on- and offshore technicians, laboratory leading officers and crew, drilling personnel, and all scientific parties are greatly acknowledged. Furthermore, B.Sc. Janne Scheffler is thanked for her excellent work in the laboratories preparing ash-bearing samples. Funding for this research was provided by the German Research Foundation (DFG) by Grants KU2685/11-1 and 11-2 associated with the DFG IODP priority program. J.L. Hopkins acknowledges the NZ Marsden Fund Te Pūta Rangahau a Marsden for supporting her Marsden Fast Start project, "Cryptotephra: unearthing hidden eruptions from the Taupō Volcanic Zone" (MFP-VUW1809). The authors wish to acknowledge funding support from L. Strachan's NZ Marsden Fund Te Pūta Rangahau a Marsden project, "Does climate influence the frequency of volcanic activity and earthquakes?" (MFP-20-UOA-099). The authors would like to thank Julie C. Belo and Phil Barnes for their reviews and suggestions.

References

Allan, A.S.R., Baker, J.A., Carter, L., and Wysoczanksi, R.J., 2008. Reconstructing the Quaternary evolution of the world's most active silicic volcanic system: insights from an ~1.65 Ma deep ocean tephra record sourced from Taupo Volcanic Zone, New Zealand. Quaternary Science Reviews, 27(25):2341–2360. **https://doi.org/10.1016/j.quascirev.2008.09.003**

Alloway, B.V., Pillans, B.J., Carter, L., Naish, T.R., and Westgate, J.A., 2005. Onshore–offshore correlation of Pleistocene rhyolitic eruptions from New Zealand: implications for TVZ eruptive history and paleoenvironmental construction. Quaternary Science Reviews, 24(14):1601–1622. **https://doi.org/10.1016/j.quascirev.2004.07.026**

Barnes, P.M., Pecher, I.A., LeVay, L.J., Bourlange, S.M., Brunet, M.M.Y., Cardona, S., Clennell, M.B., Cook, A.E., Crundwell, M.P., Dugan, B., Elger, J., Gamboa, D., Georgiopoulou, A., Greve, A., Han, S., Heeschen, K.U., Gaowei, H., Kim, G.Y., Kitajima, H., Koge, H., Xuesen, L., Machado, K.S., McNamara, D.D., Moore, G.F., Mountjoy, J.J., Nole, M.A., Owari, S., Paganoni, M., Petronotis, K.E., Rose, P.S., Screaton, E.J., Shankar, U., Shepherd, C.L., Torres, M.E., Underwood, M.B., Xiujuan, W., Woodhouse, A.D., and Wu, H.-Y., 2019a. Site U1517. In Pecher, I.A., Barnes, P.M., LeVay, L.J., and the Expedition 372A Scientists, Creeping Gas Hydrate Slides. Proceedings of the International Ocean Discovery Program, 372A: College Station, TX (International Ocean Discovery Program). **https://doi.org/10.14379/iodp.proc.372A.103.2019**

Barnes, P.M., Wallace, L.M., Saffer, D.M., Pecher, I.A., Petronotis, K.E., LeVay, L.J., Bell, R.E., Crundwell, M.P., Engelmann de Oliveira, C.H., Fagereng, A., Fulton, P.M., Greve, A., Harris, R.N., Hashimoto, Y., Hüpers, A., Ikari, M.J., Ito, Y., Kitajima, H., Kutterolf, S., Lee, H., Li, X., Luo, M., Malie, P.R., Meneghini, F., Morgan, J.K., Noda, A., Rab-

inowitz, H.S., Savage, H.M., Shepherd, C.L., Shreedharan, S., Solomon, E.A., Underwood, M.B., Wang, M., Woodhouse, A.D., Bourlange, S.M., Brunet, M.M.Y., Cardona, S., Clennell, M.B., Cook, A.E., Dugan, B., Elger, J., Gamboa, D., Georgiopoulou, A., Han, S., Heeschen, K.U., Hu, G., Kim, G.Y., Koge, H., Machado, K.S., McNamara, D.D., Moore, G.F., Mountjoy, J.J., Nole, M.A., Owari, S., Paganoni, M., Rose, P.S., Screaton, E.J., Shankar, U., Torres, M.E., Wang, X., and Wu, H.-Y., 2019b. Site U1519. In Wallace, L.M., Saffer, D.M., Barnes, P.M., Pecher, I.A., Petronotis, K.E., LeVay, L.J., and the Expedition 372/375 Scientists, Hikurangi Subduction Margin Coring, Logging, and Observatories. Proceedings of the International Ocean Discovery Program, 372B/375: College Station, TX (International Ocean Discovery Program). **https://doi.org/10.14379/iodp.proc.372B375.104.2019**

Barnes, P.M., Wallace, L.M., Saffer, D.M., Pecher, I.A., Petronotis, K.E., LeVay, L.J., Bell, R.E., Crundwell, M.P., Engelmann de Oliveira, C.H., Fagereng, A., Fulton, P.M., Greve, A., Harris, R.N., Hashimoto, Y., Hüpers, A., Ikari, M.J., Ito, Y., Kitajima, H., Kutterolf, S., Lee, H., Li, X., Luo, M., Malie, P.R., Meneghini, F., Morgan, J.K., Noda, A., Rabinowitz, H.S., Savage, H.M., Shepherd, C.L., Shreedharan, S., Solomon, E.A., Underwood, M.B., Wang, M., Woodhouse, A.D., Bourlange, S.M., Brunet, M.M.Y., Cardona, S., Clennell, M.B., Cook, A.E., Dugan, B., Elger, J., Gamboa, D., Georgiopoulou, A., Han, S., Heeschen, K.U., Hu, G., Kim, G.Y., Koge, H., Machado, K.S., McNamara, D.D., Moore, G.F., Mountjoy, J.J., Nole, M.A., Owari, S., Paganoni, M., Rose, P.S., Screaton, E.J., Shankar, U., Torres, M.E., Wang, X., and Wu, H.-Y., 2019c. Site U1520. In Wallace, L.M., Saffer, D.M., Barnes, P.M., Pecher, I.A., Petronotis, K.E., LeVay, L.J., and the Expedition 372/375 Scientists, Hikurangi Subduction Margin Coring, Logging, and Observatories. Proceedings of the International Ocean Discovery Program, 372B/375: College Station, TX (Proceedings of the International Ocean Discovery Program). **https://doi.org/10.14379/iodp.proc.372B375.105.2019**

Carter, L., Alloway, B., Shane, P., and Westgate, J., 2004. Deep-ocean record of major late Cenozoic rhyolitic eruptions from New Zealand. New Zealand Journal of Geology and Geophysics, 47(3):481–500. **https://doi.org/10.1080/00288306.2004.9515071**

Carter, R.M., McCave, I.N., Richter, C., Carter, L., et al., 1999. Proceedings of the Ocean Drilling Program, Initial Reports, 181: College Station, TX (Ocean Drilling Program). **https://doi.org/10.2973/odp.proc.ir.181.2000**

Crundwell, M.P., and Woodhouse, A., 2022a. A detailed biostratigraphic framework for 0–1.2 Ma Quaternary sediments of north-eastern Zealandia. New Zealand Journal of Geology and Geophysics. **https://doi.org/10.1080/00288306.2022.2054828**

Crundwell, M.P., and Woodhouse, A., 2022b. Biostratigraphically constrained chronologies for Quaternary sequences from the Hikurangi margin of north-eastern Zealandia. New Zealand Journal of Geology and Geophysics. **https://doi.org/10.1080/00288306.2022.2101481**

Expedition 329 Scientists, 2011. South Pacific gyre subseafloor life. Integrated Ocean Drilling Program Preliminary Report, 329. **https://doi.org/10.2204/iodp.pr.329.2011**

Freundt, A., Schindlbeck-Belo, J.C., Kutterolf, S., and Hopkins, J.L., 2021. Tephra layers in the marine environment: a review of properties and emplacement processes. In Di Capua, A., De Rosa, R., Kereszturi, G., Le Pera, E., Rosi, M., and Watt, S.F.L. (Eds.), Volcanic Processes in the Sedimentary Record: When Volcanoes Meet the Environment. Geological Society Special Publication, 520. **https://doi.org/10.1144/SP520-2021-50**

Günther, D., Jackson, S.E., and Longerich, H.P., 1999. Laser ablation and arc/spark solid sample introduction into inductively coupled plasma mass spectrometers. Spectrochimica Acta Part B: Atomic Spectroscopy, 54(3–4):381–409. **https://doi.org/10.1016/S0584-8547(99)00011-7**

Hunt, J.B., and Hill, P.G., 2001. Tephrological implications of beam size–sample-size effects in electron microprobe analysis of glass shards. Journal of Quaternary Science, 16(2):105–117. **https://doi.org/10.1002/jqs.571**

Jarosewich, E., Nelen, J.A., and Norberg, J.A., 1980. Reference samples for electron microprobe analysis. Geostandards Newsletter, 4(1):43–47. **https://doi.org/10.1111/j.1751-908X.1980.tb00273.x**

Jochum, K.P., Weis, U., Stoll, B., Kuzmin, D., Yang, Q., Raczek, I., Jacob, D.E., Stracke, A., Birbaum, K., Frick, D.A., Günther, D., and Enzweiler, J., 2011. Determination of reference values for NIST SRM 610–617 glasses following ISO guidelines. Geostandards and Geoanalytical Research, 35(4):397–429. **https://doi.org/10.1111/j.1751-908X.2011.00120.x**

Kennett, J.P., von der Borch, C.C, et al., 1986. Initial Reports of the Deep Sea Drilling Project, 90: Washington, DC (US Government Printing Office). **https://doi.org/10.2973/dsdp.proc.90.1986**

Kutterolf, S., Freundt, A., and Burkert, C., 2011. Eruptive history and magmatic evolution of the 1.9 kyr Plinian dacitic Chiltepe tephra from Apoyeque volcano in west-central Nicaragua. Bulletin of Volcanology, 73(7):811–831. **https://doi.org/10.1007/s00445-011-0457-0**

Kutterolf, S., Freundt, A., Hansteen, T.H., Dettbarn, R., Hampel, F., Sievers, C., Wittig, C., Allen, S.R., Druitt, T.H., McPhie, J., Nomikou, P., Pank, K., Schindlbeck-Belo, J.C., Wang, K.-L., Lee, H.-Y., and Friedrichs, B., 2021. The medial offshore record of explosive volcanism along the central to eastern Aegean Volcanic Arc: 1. tephrostratigraphic correlations. Geochemistry, Geophysics, Geosystems, 22(12):e2021GC010010. **https://doi.org/10.1029/2021GC010010**

Le Maitre, R.W., Steckeisen, A., Zanettin, B., Le Bas, M.J., Bonin, B., and Bateman, P. (Eds.), 2002. Igneous Rocks: A Classification and Glossary of Terms (Second edition): Cambridge, UK (Cambridge University Press). **https://doi.org/10.1017/CBO9780511535581**

Norman, M.D., Pearson, N.J., Sharma, A., and Griffin, W.L., 1996. Quantitative analysis of trace elements in geological materials by laser ablation ICPMS: instrumental operating conditions and calibration values of NIST glasses. Geostandards Newsletter, 20(2):247–261. **https://doi.org/10.1111/j.1751-908X.1996.tb00186.x**

Pank, K., Kutterolf, S., Hopkins, J.L., Wang, K.-L., and Lee, H.-Y., 2023. Supplementary material, **https://doi.org/10.14379/iodp.proc.372B375.210supp.2023**. In Pank, K., Kutterolf, S., Hopkins, J.L., Wang, K.-L., and Lee, H.-Y., Data report: marine tephra compositions in proximal and distal drill cores, IODP Expeditions 375, 372, and 329, ODP Leg 181, and DSDP Leg 90, offshore New Zealand, Southwest Pacific. In Wallace, L.M., Saffer, D.M., Barnes, P.M., Pecher, I.A., Petronotis, K.E., LeVay, L.J., and the Expedition 372/375 Scientists, Hiku-

rangi Subduction Margin Coring, Logging, and Observatories. Proceedings of the International Ocean Discovery Program, 372B/375: College Station, TX (International Ocean Discovery Program).

Peccerillo, A., and Taylor, S.R., 1976. Geochemistry of Eocene calc-alkaline volcanic rocks from the Kastamonu area, northern Turkey. Contributions to Mineralogy and Petrology, 58(1):63–81. **https://doi.org/10.1007/BF00384745**

Pecher, I.A., Barnes, P.M., LeVay, L.J., and the Expedition 372 Scientists, 2018. Expedition 372 Preliminary Report: Creeping Gas Hydrate Slides and Hikurangi LWD: College Station, TX, United States **https://doi.org/10.14379/iodp.pr.372.2018**

Ryan, W.B.F., Carbotte, S.M., Coplan, J.O., O'Hara, S., Melkonian, A., Arko, R., Weissel, R.A., Ferrini, V., Goodwillie, A., Nitsche, F., Bonczkowski, J., and Zemsky, R., 2009. Global multi-resolution topography synthesis. Geochemistry, Geophysics, Geosystems, 10(3):Q03014. **https://doi.org/10.1029/2008GC002332**

Saffer, D.M., Wallace, L.M., Barnes, P.M., Pecher, I.A., Petronotis, K.E., LeVay, L.J., Bell, R.E., Crundwell, M.P., Engelmann de Oliveira, C.H., Fagereng, A., Fulton, P.M., Greve, A., Harris, R.N., Hashimoto, Y., Hüpers, A., Ikari, M.J., Ito, Y., Kitajima, H., Kutterolf, S., Lee, H., Li, X., Luo, M., Malie, P.R., Meneghini, F., Morgan, J.K., Noda, A., Rabinowitz, H.S., Savage, H.M., Shepherd, C.L., Shreedharan, S., Solomon, E.A., Underwood, M.B., Wang, M., Woodhouse, A.D., Bourlange, S.M., Brunet, M.M.Y., Cardona, S., Clennell, M.B., Cook, A.E., Dugan, B., Elger, J., Gamboa, D., Georgiopoulou, A., Han, S., Heeschen, K.U., Hu, G., Kim, G.Y., Koge, H., Machado, K.S., McNamara, D.D., Moore, G.F., Mountjoy, J.J., Nole, M.A., Owari, S., Paganoni, M., Rose, P.S., Screaton, E.J., Shankar, U., Torres, M.E., Wang, X., and Wu, H.-Y., 2019. Expedition 372B/375 summary. In Wallace, L.M., Saffer, D.M., Barnes, P.M., Pecher, I.A., Petronotis, K.E., LeVay, L.J., and the Expedition 372/375 Scientists, Hikurangi Subduction Margin Coring, Logging, and Observatories. Proceedings of the International Ocean Discovery Program, 372B/375: College Station, TX (Proceedings of the International Ocean Discovery Program). **https://doi.org/10.14379/iodp.proc.372B375.101.2019**

Stevens, M.T., 2010. Miocene and Pliocene silicic Coromandel Volcanic Zone tephras from ODP Site 1124-C: petrogenetic applications and temporal evolution [MS thesis]. Victoria University of Wellington, Wellington, NZ. **https://core.ac.uk/download/pdf/41336805.pdf**

van Achterberg, E., Ryan, C., Jackson, S., and Griffin, W., 2001. LA-ICP-MS in the Earth Sciences - Appendix 3, data reduction software for LA-ICP-MS. In Sylvester, P.J., Short Course. 29: St. John's, Labrador (CA) (Mineralogical Association of Canada), 239–243.

Wallace, L.M., Saffer, D.M., Petronotis, K.E., Barnes, P.M., Bell, R.E., Crundwell, M.P., Engelmann de Oliveira, C.H., Fagereng, A., Fulton, P.M., Greve, A., Harris, R.N., Hashimoto, Y., Hüpers, A., Ikari, M.J., Ito, Y., Kitajima, H., Kutterolf, S., Lee, H., Li, X., Luo, M., Malie, P.R., Meneghini, F., Morgan, J.K., Noda, A., Rabinowitz, H.S., Savage, H.M., Shepherd, C.L., Shreedharan, S., Solomon, E.A., Underwood, M.B., Wang, M., and Woodhouse, A.D., 2019. Site U1526. In Wallace, L.M., Saffer, D.M., Barnes, P.M., Pecher, I.A., Petronotis, K.E., LeVay, L.J., and the Expedition 372/375 Scientists, Hikurangi Subduction Margin Coring, Logging, and Observatories. Proceedings of the International Ocean Discovery Program, 372B/375: College Station, TX (International Ocean Discovery Program). **https://doi.org/10.14379/iodp.proc.372B375.106.2019**